Soil & Tillage Research 119 (2012) 60–69

Contents lists available at SciVerse ScienceDirect

Soil & Tillage Research

journal homepage: www.elsevier.com/locate/still

Additional scaled solutions to Richards' equation for infiltration and drainage

M. Sadeghi [a,b,*], B. Ghahraman [a], A.N. Ziaei [a], K. Davary [a], K. Reichardt [c]

[a] Department of Water Engineering, College of Agriculture, Ferdowsi University of Mashhad, Mashhad, Iran
[b] Department of Plants, Soils, and Climate, Utah State University, Logan, UT, USA
[c] Laboratory of Soil Physics, Center for Nuclear Energy in Agriculture, University of São Paulo, Piracicaba, Brazil

ARTICLE INFO

Article history:
Received 31 July 2011
Received in revised form 13 December 2011
Accepted 16 December 2011

Keywords:
Richards' equation
Invariant solutions
Warrick and Hussen
Dissimilar soils

ABSTRACT

Warrick and Hussen developed in the nineties of the last century a method to scale Richards' equation (RE) for similar soils. In this paper, new scaled solutions are added to the method of Warrick and Hussen considering a wider range of soils regardless of their dissimilarity. Gardner–Kozeny hydraulic functions are adopted instead of Brooks–Corey functions used originally by Warrick and Hussen. These functions allow to reduce the dependence of the scaled RE on the soil properties. To evaluate the proposed method (PM), the scaled RE was solved numerically using a finite difference method with a fully implicit scheme. Three cases were considered: constant-head infiltration, constant-flux infiltration, and drainage of an initially uniform wet soil. The results for five texturally different soils ranging from sand to clay (adopted from the literature) showed that the scaled solutions were invariant to a satisfactory degree. However, slight deviations were observed mainly for the sandy soil. Moreover, the scaled solutions deviated when the soil profile was initially wet in the infiltration case or when deeply wet in the drainage condition. Based on the PM, a Philip-type model was also developed to approximate RE solutions for the constant-head infiltration. The model showed a good agreement with the scaled RE for the same range of soils and conditions, however only for Gardner–Kozeny soils. Such a procedure reduces numerical calculations and provides additional opportunities for solving the highly nonlinear RE for unsaturated water flow in soils.

1. Introduction

After Miller and Miller (1956), who introduced the "similar media" concept, scaling methods were invented and have been frequently used in soil physics studies, for example, for describing soils variability in terms of soil hydraulic properties (Warrick et al., 1977; Ahuja and Williams, 1991; Kosugi and Hopmans, 1998; Shouse and Mohanty, 1998; Tuli et al., 2001; Das et al., 2005; Nasta et al., 2009; Oliveira et al., 2006; Vogel et al., 2010), or obtaining generalized solutions to a variety of soil-water phenomena (Simmons et al., 1979; Sharma et al., 1980; Shukla et al., 2002; Rasoulzadeh and Sepaskhah, 2003; Kozak and Ahuja, 2005; Roth, 2008).

One important aspect of scaling methods is to scale Richards' equation (RE) so that a single solution will suffice for numerous specific cases of water flow in a wide range of unsaturated soils. Hence, these methods considerably reduce the calculations required for heterogeneous soils (Warrick and Hussen, 1993). Some methods for scaling of RE were described by Reichardt et al. (1972), Warrick and Amoozegar-Fard (1979), Warrick et al. (1985), Sposito and Jury (1985), Vogel et al. (1991), Kutilek et al. (1991), Warrick and Hussen (1993), Nachabe (1996), Wu and Pan (1997), and Sadeghi et al. (2011). Using specific scaling factors, these methods suggest linear transformations of RE variables to achieve invariant solutions for a set of soils and/or conditions. However, satisfying the "similarity condition" for the soils and conditions is a necessity in all these methods. The similarity may be defined based on microscopic-scale geometry (Miller and Miller, 1956), shape of soil hydraulic functions (Simmons et al., 1979), or a linear variability concept (Vogel et al., 1991).

The similarity condition is difficult to truly hold in reality and will be a limitation for the application of scaling methods to real soils. Focusing on this limitation, the main objective of this study was to develop a method to scale RE applicable to dissimilar soils, considering specifically the method of Warrick and Hussen (1993). Adopting Brooks–Corey soil hydraulic models, Warrick and Hussen (1993) developed scaled solutions of RE invariant to the saturated and residual volumetric water contents, saturated hydraulic conductivity, and air-entry pressure head, as well as boundary

Abbreviations: RE, Richards' equation; PM, proposed method; WHM, Warrick–Hussen method.

* Corresponding author at: 4820 Old Main Hill, Logan, UT 84322-4820, USA. Tel.: +1 435 764 6325; fax: +1 435 797 2117.
E-mail address: morteza.sadeghi@usu.edu (M. Sadeghi).

0167-1987/$ – see front matter © 2011 Elsevier B.V. All rights reserved.
doi:10.1016/j.still.2011.12.004

or initial conditions. However, the scaled solutions were still dependent on the shape parameters of the Brooks–Corey hydraulic functions, λ and P. In other words, equality in λ and P is a requirement (i.e. the similarity condition) in this method and the scaled solutions will be invariant only for soils having equal values of λ and P. In this paper, new scaled solutions are proposed in addition to the method of Warrick and Hussen considering a wider range of soils regardless of their dissimilarity.

2. Theory

Richards' (1931) equation is obtained by combining Darcy's law, $q = -K(\partial h/\partial z - 1)$, and the mass conservation law, $\partial\theta/\partial t = -\partial q/\partial z$, which, in one-dimensional form, is written as:

$$\frac{\partial\theta}{\partial t} = \frac{\partial}{\partial z}\left(K\frac{\partial h}{\partial z} - K\right) \tag{1}$$

where q [LT^{-1}] is the water flux density, θ [L^{3}L^{-3}] the soil water content, h [L] the pressure head, K [LT^{-1}] the unsaturated hydraulic conductivity, t [T] the time, and z [L] the soil depth positive downward.

2.1. Warrick–Hussen method (WHM) for scaling RE

Warrick and Hussen (1993) adopted Brooks and Corey (1964) soil hydraulic functions as follows:

$$\theta = \theta_r + (\theta_s - \theta_r)\left(\frac{h}{h_b}\right)^{-\lambda}, \quad (h < h_b < 0) \tag{2}$$

$$K = K_s\left(\frac{\theta - \theta_r}{\theta_s - \theta_r}\right)^P \tag{3}$$

where θ_s and θ_r are the saturated and residual volumetric water contents, respectively, K_s is the saturated hydraulic conductivity, h_b is the air-entry pressure head, and λ, commonly known as pore size distribution index, and P are shape parameters. The values of λ and P are usually chosen to be related, for example, as $P = 3 + 2/\lambda$ (Brooks and Corey, 1964). These parameters are found to be correlated with some physical properties of soils. For example, assuming a fractal pore structure for soil, Tyler and Wheatcraft (1990) showed that λ is related to soil fractal dimension.

Considering a boundary or initial pressure head value of h_0 and defining $|h_0|$ as a length scaling factor, z_0, Warrick and Hussen proposed the following scaled functions and variables:

$$\theta^* = \frac{\theta - \theta_r}{\theta_0 - \theta_r} \tag{4}$$

$$h^* = \frac{h}{z_0} \tag{5}$$

$$K^* = \frac{K}{K_0} \tag{6}$$

$$z^* = \frac{z}{z_0} \tag{7}$$

$$t^* = \frac{K_0 t}{z_0(\theta_0 - \theta_r)} \tag{8}$$

where θ_0 and K_0 represent $\theta(h_0)$ and $K(h_0)$, respectively. Considering Warrick and Hussen definitions of h_0 (boundary pressure head in infiltration and initial pressure head in drainage — discussed in detail later), in this method, h^* ranges from -1 to $-\infty$ and θ^* and K^* range between 0 and 1.

Substituting the scaled functions and variables, Eqs. (4)–(8), into Eq. (1) yields a scaled form of RE as follows:

$$\frac{\partial\theta^*}{\partial t^*} = \frac{\partial}{\partial z^*}\left(K^*\frac{\partial h^*}{\partial z^*} - K^*\right) \tag{9}$$

with the following reduced forms of Brooks–Corey hydraulic functions:

$$\theta^* = (-h^*)^{-\lambda} \tag{10}$$

$$K^* = \theta^{*P} \tag{11}$$

Eq. (9) is expressed in a form independent of h_0, θ_s, θ_r, K_s, and h_b. However, λ and P are the hydraulic properties remaining in Eqs. (10) and (11) which make Eq. (9) dependent on the soil properties. Therefore, the scaled solutions will be invariant only for the similar soils with shapely similar hydraulic functions (i.e. equal values of λ and P).

2.1.1. Soil-dependency of the scaled RE of the WHM

Let us accept the relationship of $P = 3 + 2/\lambda$. Then, combining Eqs. (9)–(11) yields the governing partial differential equation of the WHM, PDE_{WH}, rearranged based on h^* as follows:

$$PDE_{WH} = F_1\frac{\partial h^*}{\partial t^*} - \frac{\partial}{\partial z^*}\left(F_2\frac{\partial h^*}{\partial z^*} - F_2\right) \tag{12}$$

where F_1 and F_2 are two P-dependent functions as follows:

$$F_1 = \frac{2}{P-3}(-h^*)^{(1-P)/(P-3)} \tag{13}$$

$$F_2 = K^* = (-h^*)^{2P/(3-P)} \tag{14}$$

The variation of PDE_{WH} in terms of P is given as follows:

$$\frac{\partial(PDE_{WH})}{\partial P} = \frac{\partial F_1}{\partial P}\frac{\partial h^*}{\partial t^*} - \frac{\partial}{\partial P}\left(\frac{\partial F_2}{\partial z^*}\right)\frac{\partial h^*}{\partial z^*} - \frac{\partial F_2}{\partial P}\frac{\partial^2 h^*}{\partial z^{*2}} + \frac{\partial}{\partial P}\left(\frac{\partial F_2}{\partial z^*}\right) \tag{15}$$

Eq. (15) elucidates the dependency of the scaled solutions of the WHM on P.

2.2. Proposed method (PM) for scaling RE

Here, Gardner's (1958) model for the hydraulic conductivity function is exploited:

$$K = K_s\exp\left(-\frac{h}{h_{cM}}\right) \tag{16}$$

where h_{cM} is the effective capillary drive introduced by Morel-Seytoux and Khanji (1974) as $h_{cM} = 1/K_s\int_0^\infty K(h)dh$. To find a proper water retention model corresponding to Eq. (16), we use Eq. (3) which, in fact, is Kozeny's equation (adopted from Mualem, 1976) and yields the following water retention model when combined with Eq. (16):

$$\theta = \theta_r + (\theta_s - \theta_r)\exp\left(-\frac{h}{Ph_{cM}}\right) \tag{17}$$

Eqs. (16) and (17) may be referred to as Gardner–Kozeny hydraulic functions (Bakker and Nieber, 2009). Assuming $P = 1$, Gardner–Kozeny functions yield the functions widely used in the literature for linearization of RE in order to analytically solve it (Warrick, 1975; Chen et al., 2001; Tracy, 2007). However, the assumption of $P = 1$ is difficult to hold in real soils (see values of P for the soils studied here in Table 1), and considering the general form of Gardner–Kozeny functions with P as a fitting parameter is more realistic.

Table 1
Brooks–Corey and Gardner–Kozeny hydraulic parameters of the selected soils.

Soil name	P[a]	θ_r	θ_s	h_b (cm)	h_{cM} (cm)	K_s (cm/day)
Upland sand	7.66	0	0.305	−6.31	−6.33	186.0
Rubicon sandy loam	12.08	0	0.380	−6.39	−12.66	28.8
Fukushima loam	13.32	0	0.755	−9.23	−8.37	473.5
Yolo light clay	16.82	0	0.495	−7.52	−21.74	1.06
Columbia silt loam	19.00	0	0.401	−15.95	−40.00	5.04

[a] P was taken as $3+2/\lambda$.

We assume in the PM that $z_0 = |h_{cM}|$. To scale RE for infiltration, Nachabe (1996) used the macroscopic capillary length, λ_s, as the length scaling factor which has a nearly similar definition ($\lambda_s = 1/(K_0 - K_i)\int_{h_i}^{h_0} K(h)dh$, where h_i is the initial pressure head and K_i is $K(h_i)$). When $h_0 = 0$ and $h_i \to -\infty$, λ_s approaches h_{cM}. However, h_{cM} is a static property and constant for each soil, while h_0 and λ_s are dynamic properties of a soil and dependent on the boundary and initial conditions.

We define in the PM the following scaled pressure head:

$$h^* = \frac{h - h_0}{z_0} \tag{18}$$

ranging from 0 to $-\infty$ (considering Warrick and Hussen definitions of h_0). Applying $z_0 = |h_{cM}|$, the other scaled functions and variables are kept the same as defined in Eqs. (5)–(8). Substituting the proposed scaled functions and variables into Eq. (1), the resulting scaled RE remains in the form of Eq. (9), however; the following reduced hydraulic functions are applied instead of Eqs. (10) and (11):

$$K^* = \exp(h^*) \tag{19}$$

$$\theta^* = \exp\left(\frac{h^*}{P}\right) \tag{20}$$

2.2.1. Soil-dependency of the PM for the scaled RE

Combining Eqs. (9), (19), and (20) yields the governing partial differential equation of the proposed method, PDE_P, rearranged based on h^* as follows:

$$PDE_P = F_3\frac{\partial h^*}{\partial t^*} - \frac{\partial}{\partial z^*}\left[\exp(h^*)\left(\frac{\partial h^*}{\partial z^*} - 1\right)\right] \tag{21}$$

where

$$F_3 = \frac{1}{P}\exp\left(\frac{h^*}{P}\right) \tag{22}$$

The soil-dependency of the PM for the scaled RE can be evaluated by differentiating PDE_P with respect to P as follows:

$$\frac{\partial(PDE_P)}{\partial P} = \frac{\partial F_3}{\partial P}\frac{\partial h^*}{\partial t^*} \tag{23}$$

Three terms containing F_2 in Eq. (15) have been removed by applying the PM. The only remaining term in Eq. (23) is analogous to the first term of Eq. (15). The factors $\partial F_1/\partial P$ and $\partial F_3/\partial P$ in these terms are obtained from Eqs. (13) and (22), respectively, as follows:

$$\frac{\partial F_1}{\partial P} = \left[\frac{6 - 2P + 4\ln(-h^*)}{(P-3)^3}\right](-h^*)^{(1-p)/(p-3)} \tag{24}$$

$$\frac{\partial F_3}{\partial P} = \left(\frac{-P - h^*}{P^3}\right)\exp\left(\frac{h^*}{P}\right) \tag{25}$$

The behavior of Eqs. (24) and (25) at different values of P and h^* has been depicted in Fig. 1. This figure shows that for identical values of P and h^*, $\partial F_1/\partial P$ is greater than $\partial F_3/\partial P$ particularly at lower values of $|h^*|$ (i.e. near saturation). This means that the total P-dependency of PDE_p is lower than that of PDE_{WH} due to the first term of Eq. (15).

Fig. 1 also shows that $\partial F_3/\partial P$ generally increases as P decreases indicating that the P-dependency of the PDE_p is higher in coarser textures (lower P) in comparison to those of finer textures (higher P). In addition, $\partial F_3/\partial P$ decreases as $|h^*|$ increases (i.e. soil becomes drier). When $|h^*|$ becomes greater than about 100, $\partial F_3/\partial P$ approaches zero for most soils and thus, PDE_p becomes approximately soil-independent.

3. Materials and methods

Five texturally different soils were selected from the literature in order to cover a wide texture range especially with respect to P—the only influencing parameter on the scaled solutions of RE in both methods. The soil properties including Brooks–Corey and Gardner–Kozeny hydraulic parameters, presented in Table 1, were obtained by fitting the data presented in Figs. 1 and 4 of Kawamoto et al. (2006).

To show the improvements of the PM to scale RE, Warrick and Hussen (1993) evaluations were repeated for both methods. Eq. (9) was solved numerically with the scaled hydraulic functions of (10) and (11) for the WHM and (19) and (20) for the PM. The numerical calculations were performed using the finite difference method with the fully implicit scheme identical to that of HYDRUS-1D (Simunek et al., 2005). To do so, a computer code was written in MATLAB. Similar to Warrick and Hussen (1993), three test cases were considered: (1) infiltration with a constant pressure head at

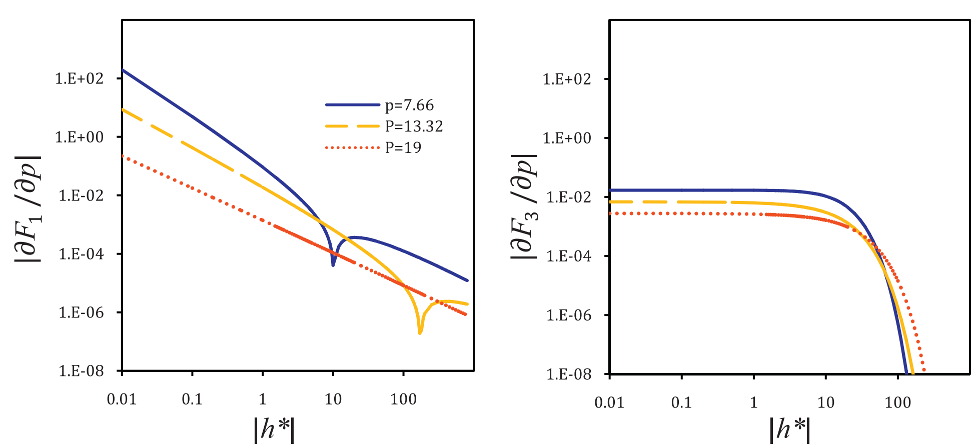

Fig. 1. Description of the factors $\partial F_1/\partial P$ and $\partial F_3/\partial P$ of Eqs. (24) and (25) as a function of the scaled pressure head.

Table 2
Boundary and initial conditions in the three test cases.

Case	Upper boundary	Lower boundary	Initial
Constant-head infiltration	$h = h_0$	$h = h_i$	$h = h_i$
Constant-flux infiltration	$q = K_0$	$h = h_i$	$h = h_i$
Drainage	$q = 0$	Free drainage ($q = K$)	$h = h_0$ ($z < L$)

the soil surface into a uniform dry soil, (2) infiltration with a constant flux density at the soil surface into a uniform dry soil, and (3) drainage of a uniformly wet soil with no flow at the soil surface. Regarding boundary and initial conditions for each process, we defined h_0 in a similar way as Warrick and Hussen (1993) did. Table 2 summarizes the boundary and initial conditions in the three cases. In this table, h_i is the initial pressure head in infiltration, and L is the length of the soil column in drainage.

Considering Darcy's law, $q = -K(\partial h/\partial z - 1)$, Eqs. (4), (6), and (7) (for the WHM) or (18), (6), and (19) (for the PM) suggest the following scaled flux density, q^*, in both methods:

$$q^* = \frac{q}{K_0} \tag{26}$$

Applying Eqs. (4), (6), (7), and (26), scaled boundary and initial conditions as presented in Table 3 are attained. The scaled lower boundary and initial conditions in infiltration, h_i^*, and the scaled length of the soil column in drainage, L^*, influence the scaled solutions in both methods. However, other scaled boundary and initial conditions are invariant.

4. Results and discussion

4.1. Constant-head infiltration

Scaled solutions of the WHM for the constant-head infiltration with $h_i^* = -100$ are presented in Fig. 2. The figure shows plot of the scaled pressure head versus the scaled depth at two scaled times of 0.1 and 1 (For $h_0 = h_b$, the scaled time of 0.1 is corresponding to the real time of 1.49 and 505.44 min for the Upland sand and Yolo light clay, respectively). Due to the wide range of P for the selected soils, the scaled solutions of the WHM are significantly different (Fig. 2). This is confirmed by the high CV values appearing in the figure, which represent an average of the variation coefficients of h^* along the wet zone.

Since the WHM is expected to give invariant scaled solutions for similar soils (i.e. with equal values of P), these selected soils (with P values having a coefficient of variation of about 32%) indicate a high degree of dissimilarity. As expected, the scaled solutions are nearly invariant for soils with close values of P (e.g. Rubicon sandy loam and Fukushima loam) which approximately preserve the similarity condition.

The high degree of dissimilarity of the selected soils gives an opportunity to seriously evaluate the PM. Fig. 3 shows the scaled solutions of the PM for the constant-head infiltration with $h_i^* = -100$. The scaled pressure head profiles are shown at two scaled times of 0.1 and 1 (Assuming $h_0 = 0$, the scaled time of 0.1 corresponds the real time of 1.49 and 1461.21 min for the Upland sand and Yolo light clay, respectively). Although the soils are completely dissimilar, Fig. 3 indicates that the scaled solutions are nearly invariant for all the soils and show a unified curve. For the

Table 3
Scaled boundary and initial conditions in the three test cases.

Case	Warrick–Hussen method			Proposed method		
	Upper boundary	Lower boundary	Initial	Upper boundary	Lower boundary	Initial
Constant-θ infiltration	$h^* = 1$	$h^* = h_i^*$	$h^* = h_i^*$	$h^* = 0$	$h^* = h_i^*$	$h^* = h_i^*$
Constant-flux infiltration	$q^* = 1$	$h^* = h_i^*$	$h^* = h_i^*$	$q^* = 1$	$h^* = h_i^*$	$h^* = h_i^*$
Drainage	$q^* = 0$	$q^* = K^*$	$h^* = 1$ ($z^* < L^{*a}$)	$q^* = 0$	$q^* = K^*$	$h^* = 0$ ($z^* < L^*$)

[a] $L^* = L/z_0$.

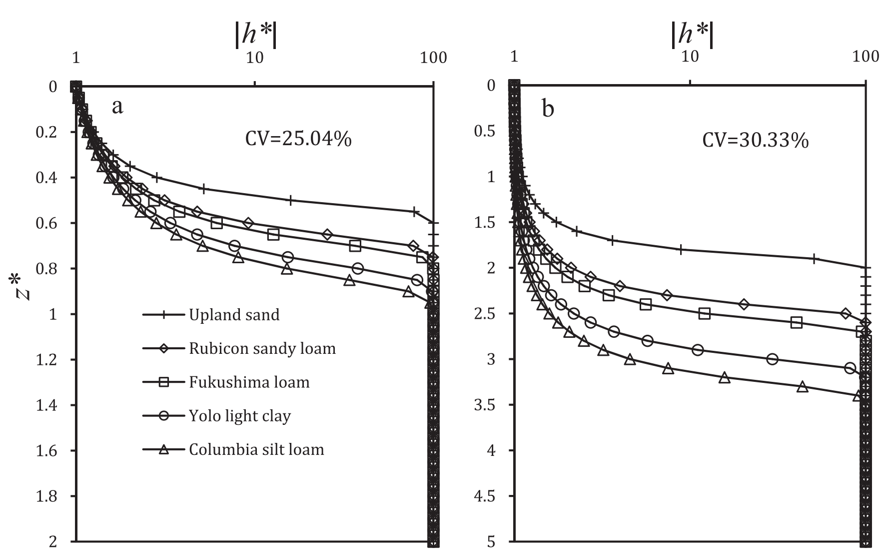

Fig. 2. Scaled pressure head versus scaled depth obtained using the Warrick–Hussen (WHM) method for constant-head infiltration with scaled initial pressure head of −100 at (a) $t^* = 0.1$ and (b) $t^* = 1$.

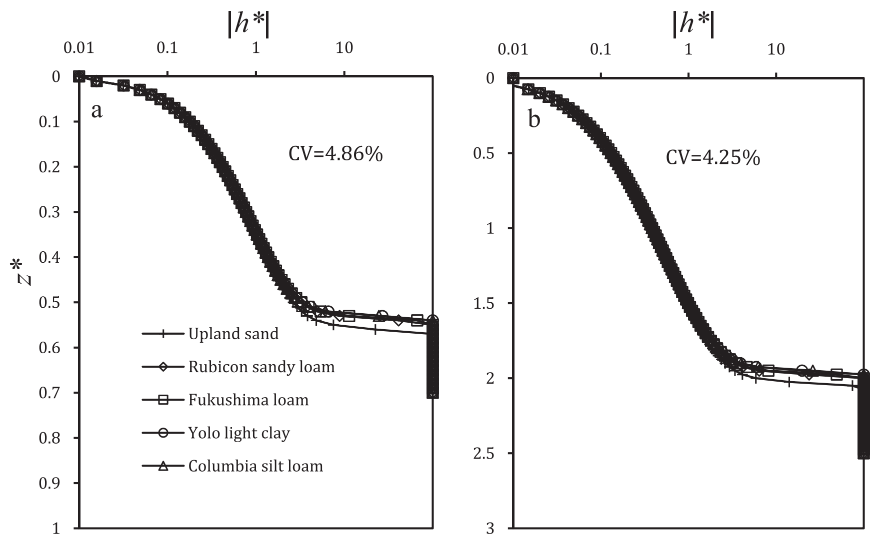

Fig. 3. Scaled pressure head versus scaled depth obtained using proposed method (PM) for constant-head infiltration with scaled initial pressure head of −100 at (a) t^* = 0.1 and (b) t^* = 1.

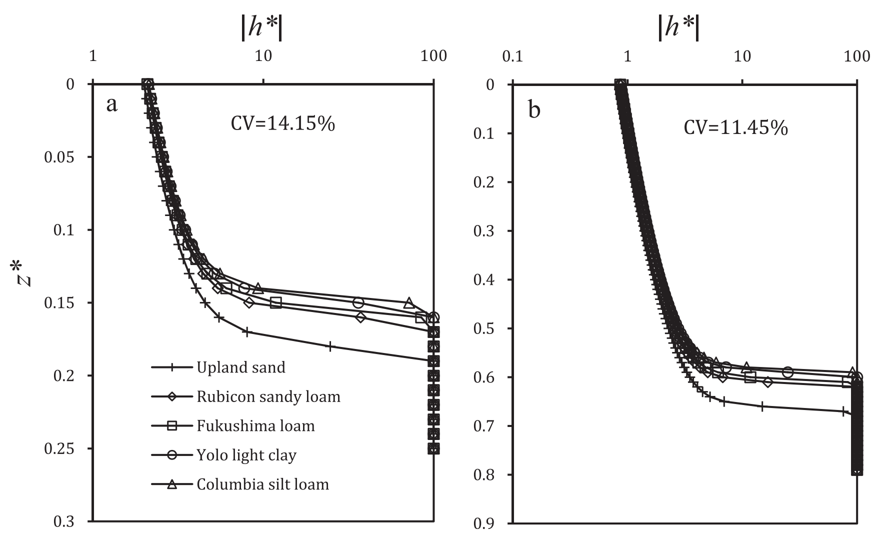

Fig. 4. Scaled pressure head versus scaled depth obtained using proposed method (PM) for constant-flux infiltration with scaled initial pressure head of −100 at (a) t^* = 0.1 and (b) t^* = 0.5.

Upland sand, a slight deviation exists which is due to the greater P-dependency of F_3 (i.e. greater values of $\partial F_3/\partial P$) for lower values of P as shown in Fig. 1.

4.2. Constant-flux infiltration

Scaled solutions of the WHM for the constant-flux infiltration (not presented here) also were significantly different for the five soils (For the case of $h_i^* = -100$, CV was 30.33% at t^* = 0.5). In contrast, for the same case, the scaled solutions of the PM except for the Upland sand were close to each other as presented in Fig. 4 (by removing the Upland sand, CV becomes 7.44% and 5.72% for Fig. 4a and b, respectively). CV decreases with time in this case. Such a result can be due to the sudden decrease of $\partial h^*/\partial t^*$ during the constant-flux infiltration which decreases the soil-dependency of the scales solutions according to Eq. (23).

4.3. Drainage

Scaled results of the WHM are presented in Fig. 5 for the drainage in a profile with scaled depth of L^* = 1. The scaled pressure head profiles are shown at two scaled times of 1 and 10. The CV values deal with the variations of the scaled solutions for the five soils. Comparing this figure with the scaled solutions of the PM as shown in Fig. 6, it can be seen that the PM significantly reduces the CV values. As Fig. 6 indicates, the scaled solutions of the PM become closer by passing the time. According to Eq. (23), this is justified by the decrease of both $\partial F_3/\partial P$ (see Fig. 1) and $\partial h^*/\partial t^*$ during the drainage process.

4.4. Effect of the data quality

The fitting parameter P, which affects the scaled solutions, is not only changed by soil texture, but also by measurement errors of the hydraulic properties. Hence, the scaled solutions can be affected by measurement accuracy. To evaluate this effect, we considered Eq. (3) containing an error parameter, ε, in the form of $K_r = (S_e + \varepsilon)^P$, where K_r is the relative hydraulic conductivity, and S_e the effective degree of saturation. We assumed ε as a normally distributed random error with the mean of zero and standard deviation of σ. Firstly, applying P = 13.32 (that of the Fukushima loam) to the relationship of $K_r = S_e^P$, we generated a standard set of $K_r - S_e$ data

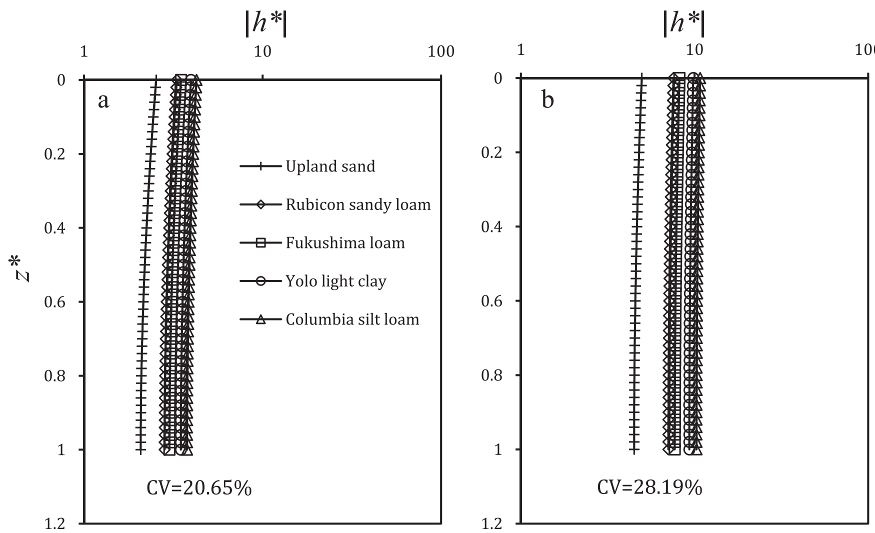

Fig. 5. Scaled pressure head versus scaled depth obtained using Warrick–Hussen method (WHM) for drainage in a profile with scaled depth of 1 at (a) $t^* = 1$ and (b) $t^* = 10$.

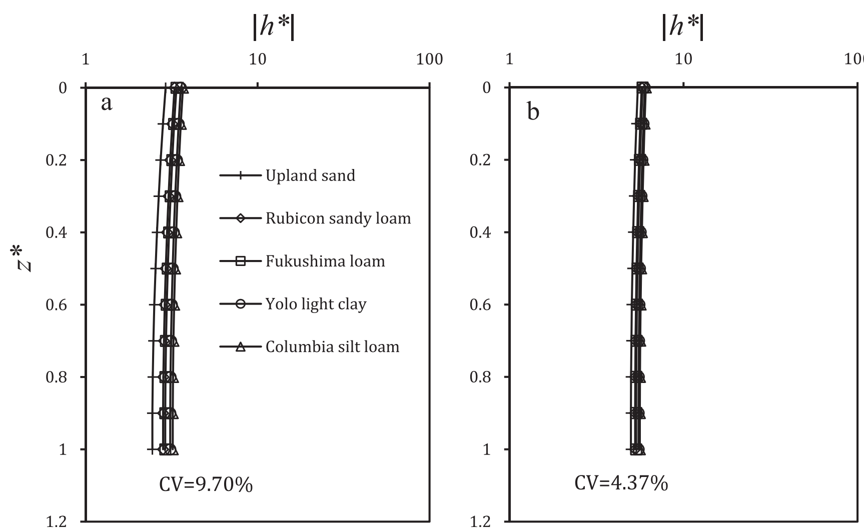

Fig. 6. Scaled pressure head versus scaled depth obtained using proposed method (PM) for drainage in a profile with scaled depth of 1 at (a) $t^* = 1$ and (b) $t^* = 10$.

by changing S_e from zero to unity. Then, by assuming different values of σ as 0.01, 0.02, 0.03, 0.04, and 0.05, and considering ten replications for each σ, we generated fifty sets of ε values and added them to the standard data set. Then, we refitted the relationship of $K_r = S_e^P$ to each data set and obtained fifty new P values (ranging from 11.77 to 14.37). Applying these values of P, we solved the scaled RE of both methods for the case of constant-head infiltration into the Fukushima loam assuming $h_i^* = -100$.

The solutions (not presented here) showed significant variations for the WHM, while they were invariant for the PM (CV of the fifty solutions at $t^* = 1$ was obtained 15.29% for the WHM and 0.84% for the PM). An insight to the effect of the data quality on the scaled solutions can be achieved by the results presented in Fig. 7. This figure shows the effect of the error magnitudes (in terms of σ) on the CV of the scaled solutions calculated for each of the ten replications of σ. For both methods, CV almost linearly increases as σ increases. However, the rate of this increase for the WHM is much (almost twelve times) more than that of the PM.

Note that we assumed here that the measurement error is a random variable around the Brooks–Corey or Gardner–Kozeny hydraulic models. If this condition is not met for any soil (i.e. the errors show a correlation with the hydraulic variables), that soil

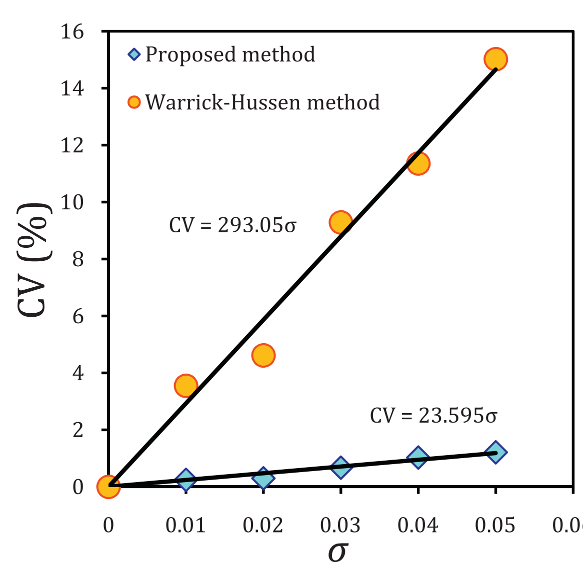

Fig. 7. Effect of σ (standard deviation of the normal distributions of the generated errors) on CV of the scaled solutions (at $t^* = 1$) calculated for each of the ten replications of σ.

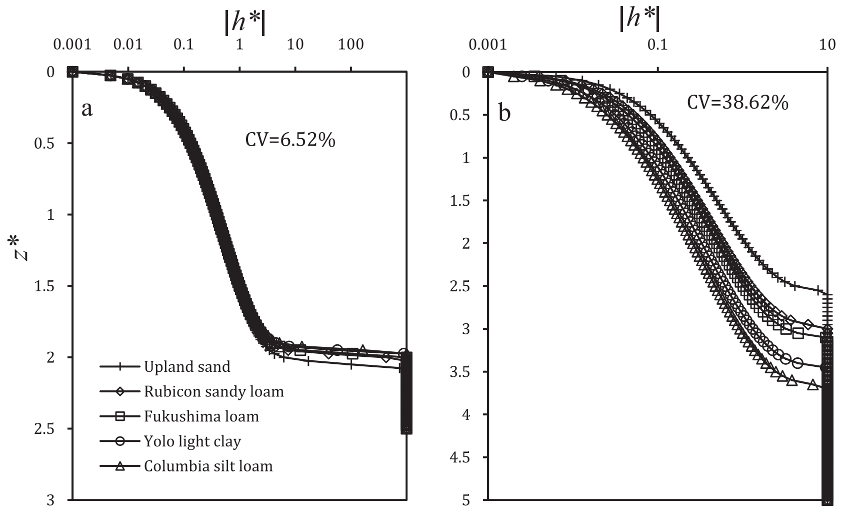

Fig. 8. Scaled pressure head versus scaled depth obtained using proposed method (PM) for constant-head infiltration with scaled initial pressure head of (a) −1000 and (b) −10 at $t^* = 1$.

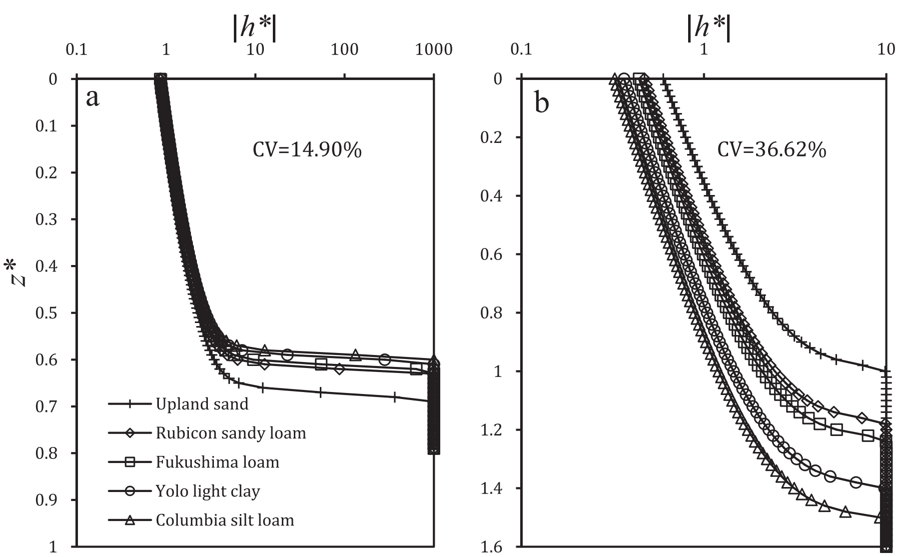

Fig. 9. Scaled pressure head versus scaled depth obtained using proposed method (PM) for constant-flux infiltration with scaled initial pressure head of (a) −1000 and (b) −10 at $t^* = 0.5$.

cannot be considered as a Brooks–Corey or Gardner–Kozeny soil and the scaling methods will not work in such condition.

4.5. Effect of the initial conditions

As mentioned earlier, the scaled solutions of the PM are dependent on the initial conditions. In other words, the primary requirement for invariance of the scaled solutions for a group of soils is that the scaled initial conditions should be identical. Here, the effects of the initial conditions on the scaled solutions are discussed.

Showing the PM results for the constant-head infiltration, Fig. 8 reveals that the scaled solutions results deviate when the initial head represents a wet condition. This result is expected in accordance to Fig. 1 in which $\partial F_3/\partial P$ gets its maximum value when $|h^*|$ reaches less than 10.

The effect of the initial conditions for the constant-flux infiltration can be evaluated by comparing Figs. 9a, 4b, and 9b in which h_i^* of -1000, -100, and -10 were considered, respectively. The lowest CV is for the case of $h_i^* = -100$ and the h^* profiles diverge in both drier and wetter conditions. The increase of the CV for the wetter profile is expected as discussed above for Fig. 8b, and for the drier profile in Fig. 9b was found to be due to the factor $\partial h^*/\partial t^*$ which is greater in this case than that of Fig. 4b.

Effect of the scaled depth of the soil profile in the drainage process is evaluated in Fig. 10. The h^* profiles are shown at $t^* = 10$ where two scaled depths were considered; 0.1 and 5. Based on this figure together with Fig. 6b, it can be concluded that the scaled solutions are more dependent on the soil properties for longer soil columns. The reason is that when the soil profile is more deeply wetted, the drainage process will be slower. Thus, at a specific scaled time, the soil profile will be wetter and both of the influencing factors ($\partial F_3/\partial P$ and $\partial h^*/\partial t^*$) will be greater.

4.6. Approximate solutions of RE for constant-head infiltration

It was found that, for the constant-head infiltration, the scaled cumulative infiltrated water curves using the PM were invariant

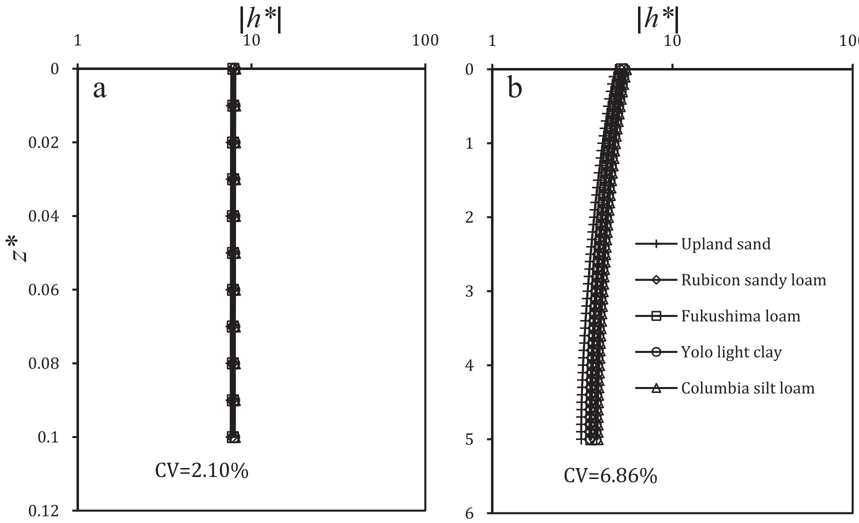

Fig. 10. Scaled pressure head versus scaled depth obtained using proposed method (PM) for drainage in a profile with scaled depth of (a) 0.1 and (b) 5 at $t^* = 10$.

for all values of h_i^* smaller than -100 (i.e. initially dry soils). This gave an opportunity to approximate RE solutions for the constant-head infiltration.

The following definition of cumulative infiltrated water, I [L], was considered:

$$I = \int_0^t q_0 \ dt \tag{27}$$

where q_0 is the surface flux (infiltration rate). Substituting Eqs. (8) and (26) into Eq. (27), a scaled cumulative infiltrated water, I^*, was calculated for the PM as:

$$I^* = \frac{I}{z_0(\theta_0 - \theta_r)} \tag{28}$$

We solved the scaled RE (Eq. (9)) for the five soils and for various h_i^* (-100, -500, -1000 and -5000). The solutions were invariant

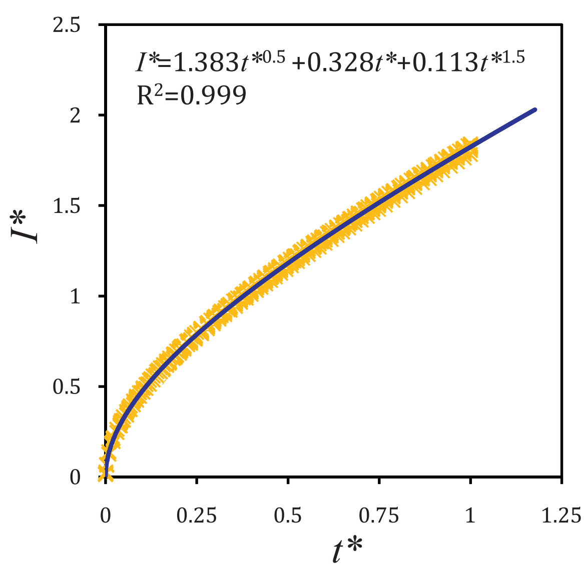

Fig. 11. Scaled cumulative infiltrated water versus scaled time obtained using proposed method (PM) for constant-head infiltration with scaled initial pressure heads of -100, -500, -1000 and -5000. Solid line shows the presented fitted curve, Eq. (30).

for all the 20 cases as shown in Fig. 11. To describe the solutions by a single curve, Philip's (1969) infiltration solution for Eq. (9) was considered in a scaled form as follows (Warrick et al., 1985):

$$I^* = At^{*^{0.5}} + Bt^* + Ct^{*^{1.5}} + \ldots \tag{29}$$

where A, B, and C and any additional term are dimensionless forms of the Philip's original solution parameters. Choosing the first three terms of the series, the following model was obtained using the least squares fitting ($R^2 = 0.999$):

$$I^* = 1.383t^{*^{0.5}} + 0.328t^* + 0.113t^{*^{1.5}} \tag{30}$$

Therefore, a single set of A, B, and C could adequately describe the scaled solutions. This can give an insight to the generality of the PM when compared with the nearly similar procedure of Warrick et al. (1985). They introduced a scaled form of Philip's solution so that A, B, and C could be tabulated for various soils and conditions.

Substituting Eqs. (8) and (28) into Eq. (30), the following model was achieved:

$$I = at^{0.5} + bt + ct^{1.5} \tag{31}$$

with

$$a = 1.383[K_0|h_{cM}|(\theta_0 - \theta_r)]^{0.5} \tag{32}$$

$$b = 0.328K_0 \tag{33}$$

$$c = 0.113K_0^{1.5}[|h_{cM}|(\theta_0 - \theta_r)]^{-0.5} \tag{34}$$

Eq. (31) introduces a Philip-type infiltration model. In this model, $K_0 = K(h_0)$ and $\theta_0 = \theta(h_0)$ can be calculated by Eqs. (16) and (17), respectively. Therefore, h_0 appears implicitly in Eq. (31) through K_0 and θ_0. However, it is limited to the values smaller than zero, because Eqs. (16) and (17) cannot account for positive heads. Therefore, Eq. (31) is valid for Gardner–Kozeny (Eqs. (16) and (17)) soils, non-positive values of h_0, and h_i^* approximately smaller than -100 (i.e. an initially dry soil).

It should be noted that for large times, the infiltration process is dominated by gravitational force and the series of Eq. (29) will diverge. Philip (1969) suggested the series is valid for $t < t_g$ where

$$t_g = [a/(K_0 - K_i)]^2 \tag{35}$$

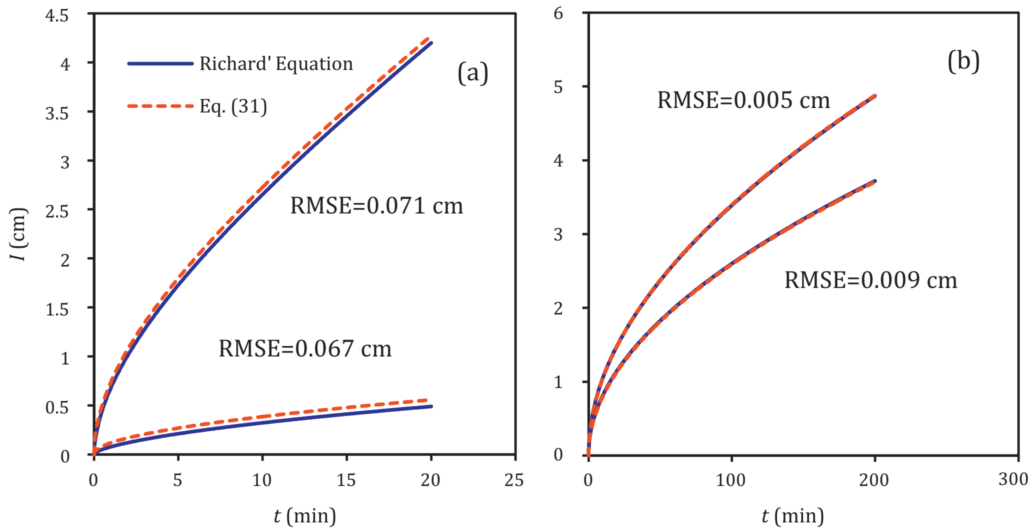

Fig. 12. Cumulative infiltration versus time obtained using Eq. (31) and numerical solution of Richards' equation with constant head of 0 (the upper curve) and −20 cm (the lower curve) and initial pressure head of −10,000 cm for (a) Upland sand and (b) Columbia silt loam.

For $t > t_g$, the infiltration rate will be K_0 (i.e. scaled infiltration rate will be unity) and I will be:

$$I = I(t_g) + (t - t_g)K_0 \tag{36}$$

To evaluate the accuracy of Eq. (31), for $t < t_g$, we compared the values of cumulative infiltrated water as approximations of Eq. (31) to RE (Eq. (1)) solutions for the Upland sand, and Columbia silt loam (as two extremely different soils regarding P) each for $h_0 = 0$ and -20 cm, and $h_i = -10{,}000$ cm (by which the condition $h_i^* \leq -100$ is met). The comparisons can be seen in Fig. 12. The figure shows a good agreement between Eq. (31) and RE which is indicated by the Root mean squared error (RMSE) values appearing in the figure. The degree of accuracy in the Columbia silt loam is higher than that of the Upland sand. The larger errors of this soil are due to the fitting error of Eq. (30). Although this error is very small, it is magnified when the scaled infiltrated water is converted to the real scale.

5. Conclusions

Warrick and Hussen (1993) developed a method to scale Richards' equation (RE) for similar soils. Here, additional scaled solutions have been developed. The advantage of the proposed method over Warrick–Hussen method is that the proposed scaled solutions are invariant for a wider range of soils regardless of their dissimilarity. The disadvantage of the proposed method is that it applies for Gardner–Kozeny functions which have a more limited applicability to soils relative to Brooks–Corey functions used in the Warrick–Hussen method. Perhaps, future studies can involve other forms of the hydraulic functions.

Using the proposed method, a Philip-type model, Eq. (31), has been developed to approximate constant-negative head infiltration. The model showed a good agreement with RE for a wide range of soils (from sand to clay) and various boundary conditions, but only for Gardner–Kozeny soils. The method is promising to reduce complicated numerical calculations and opens a new window to easily obtain approximate solutions of the highly nonlinear RE for water flow in unsaturated soils, within prescribed levels of error.

Acknowledgments

We gratefully acknowledge professors A.W. Warrick, D.R. Nielsen, and A.R. Sepaskhah for their thorough review and helpful comments.

References

Ahuja, L.R., Williams, R.D., 1991. Scaling water characteristic and hydraulic conductivity based on Gregson–Hector–McGowan approach. Soil Sci. Soc. Am. J. 55, 308–319.
Bakker, M., Nieber, J.L., 2009. Damping of sinusoidal surface flux fluctuations with soil depth. Vadose Zone J. 8, 119–126.
Brooks, R.H., Corey, A.T., 1964. Hydraulic properties of porous media. Hydrolo. Paper 3, Colorado State Univ., Fort Collins.
Chen, J.M., Tan, Y.C., Chen, C.H., Parlange, J.Y., 2001. Analytical solutions for linearized Richards equation with arbitrary time-dependent surface fluxes. Water Resour. Res. 37 (4), 1091–1093.
Das, B.S., Haws, W.N., Rao, P.S.C., 2005. Defining geometric similarity in soils. Vadose Zone J. 4, 264–270.
Gardner, W.R., 1958. Some steady-state solutions of the unsaturated moisture flow equation with application to evaporation from a water table. Soil Sci. 85, 228–232.
Kawamoto, K., Moldrup, P., Ferré, T.P.A., Tuller, M., Komatsu, T., 2006. Linking the Gardner and Campbell models for water retention and hydraulic conductivity in near-saturated soil. Soil Sci. 171, 573–584.
Kosugi, K., Hopmans, J.W., 1998. Scaling water retention curves for soils with lognormal pore-size distribution. Soil Sci. Soc. Am. J. 62, 1496–1504.
Kozak, J.A., Ahuja, L.R., 2005. Scaling of infiltration and redistribution of water across soil textural classes. Soil Sci. Soc. Am. J. 69, 816–827.
Kutilek, M., Zayani, K., Haverkamp, R., Parlange, J.Y., Vachaud, G., 1991. Scaling of Richards' equation under invariant flux boundary conditions. Water Resour. Res. 27, 2181–2185.
Miller, E.E., Miller, R.D., 1956. Physical theory for capillary flow phenomena. J. Appl. Phys. 27, 324–332.
Morel-Seytoux, H.J., Khanji, J., 1974. Derivation of an equation of infiltration. Water Resour. Res. 10, 795–800.
Mualem, Y., 1976. A new model for predicting the hydraulic conductivity of unsaturated porous media. Water Resour. Res. 12, 513–522.
Nachabe, M.H., 1996. Macroscopic capillary length, sorptivity, and shape factor in modeling the infiltration rate. Soil Sci. Soc. Am. J. 60, 957–962.
Nasta, P., Kamai, T., Chirico, G.B., Hopmans, J.W., Romano, N., 2009. Scaling soil water retention functions using particle-size distribution. J. Hydrol. 374, 223–234.
Oliveira, L.I., Demond, A.H., Abriola, L.M., Goovaerts, P., 2006. Simulation of solute transport in a heterogeneous vadose zone describing the hydraulic properties using a multistep stochastic approach. Water Resour. Res. 42, W05420, doi:10.1029/2005WR004580.
Philip, J.R., 1969. Theory of infiltration. Adv. Hydrosci. 5, 215–296.
Rasoulzadeh, A., Sepaskhah, A.R., 2003. Scaled infiltration equations for furrow irrigation. Biosys. Eng. 86, 375–383.
Reichardt, K., Nielsen, D.R., Biggar, J.W., 1972. Scaling of horizontal infiltration into homogeneous soils. Soil Sci. Soc. Am. J. Proc. 36, 241–245.
Richards, L.A., 1931. Capillary conduction of liquids through porous mediums. Physics 1, 318–333.
Roth, K., 2008. Scaling of water flow through porous media and soils. Eur. J. Soil Sci. 59, 125–130.
Sadeghi, M., Ghahraman, B., Davary, K., Hasheminia, S.M., Reichardt, K., 2011. Scaling to generalize a single solution of Richards' equation for soil water redistribution. Sci. Agric. (Piracicaba, Braz.) 68, 582–591.
Sharma, M.L., Gander, G.A., Hunt, C.G., 1980. Spatial variability of infiltration in a watershed. J. Hydrol. 45, 101–122.

Shouse, P.J., Mohanty, B.P., 1998. Scaling of near-saturated hydraulic conductivity measured using disc infiltrometers. Water Resour. Res. 34, 1195–1205.
Shukla, M.K., Kastanek, F.G., Nielsen, D.R., 2002. Inspectional analysis of convective-dispersion equation and application on measured breakthrough curves. Soil Sci. Soc. Am. J. 66, 1087–1094.
Simmons, C.S., Nielsen, D.R., Biggar, J.W., 1979. Scaling of field-measured soil-water properties. Hilgardia 47, 77–173.
Simunek, J., van Genuchten, M.Th., Sejna, M., 2005. The HYDRUS-1D Software Package for Simulating the Movement of Water, Heat, and Multiple Solutes in Variably Saturated Media. Version 3.0. HYDRUS Softw. Ser. 1. Dep. of Environ. Sci., Univ. of California, Riverside.
Sposito, G., Jury, W.A., 1985. Inspectional analysis in the theory of water flow through unsaturated soils. Soil Sci. Soc. Am. J. 49, 791–798.
Tracy, F.T., 2007. Three-dimensional analytical solutions of Richards' equation for a box-shaped soil sample with piecewise-constant head boundary conditions on the top. J. Hydrol. 336, 39–400.
Tuli, A., Kosugi, K., Hopmans, J.W., 2001. Simultaneous scaling of soil water retention and unsaturated hydraulic conductivity functions assuming lognormal pore-size distribution. Adv. Water Resour. 24, 677–688.
Tyler, S.W., Wheatcraft, S.W., 1990. Fractal processes in soil water retention. Water Resour. Res. 26, 1047–1054.
Vogel, T., Cislerova, M., Hopmans, J.W., 1991. Porous media with linearly hydraulic properties. Water Resour. Res. 27, 2735–2741.
Vogel, H.J., Weller, U., Ippisch, O., 2010. Non-equilibrium in soil hydraulic modelling. J. Hydrol. 393, 20–28.
Warrick, A.W., 1975. Analytical solutions to the one-dimensional linearized moisture flow equation for arbitrary input. Soil Sci. 120 (2), 79–84.
Warrick, A.W., Mullen, G.J., Nielsen, D.R., 1977. Scaling of field measured hydraulic properties using a similar media concept. Water Resour. Res. 13, 355–362.
Warrick, A.W., Amoozegar-Fard, A., 1979. Infiltration and drainage calculations using spatially scaled hydraulic properties. Water Resour. Res. 15, 1116–1120.
Warrick, A.W., Lomen, D.O., Yates, S.R., 1985. A generalized solution to infiltration. Soil Sci. Soc. Am. J. 49, 34–38.
Warrick, A.W., Hussen, A.A., 1993. Scaling of Richards' equation for infiltration and drainage. Soil Sci. Soc. Am. J. 57, 15–18.
Wu, L., Pan, L., 1997. A generalized solution to infiltration from single-ring infiltrometers by scaling. Soil Sci. Soc. Am. J. 61, 1318–1322.